Characterization of reciprocity gaps from interference tests in fractured media through a dual porosity model

X. Sanchez-Vila[1], P. Ackerer[2], F. Delay[2], A. Guadagnini[3,4]

[1]Hydrogeology Group (GHS), Dept of Civil and Environmental Engineering, Jordi Girona 1-3, 08034 Barcelona, Spain

[2]Laboratoire d'Hydrologie et de Géochimie de Strasbourg, Univ. Strasbourg/EOST, CNRS UMR 7517, 1 rue Blessig, 67084 Strasbourg, France

[3]Dipartimento di Ingegneria Civile e Ambientale, Politecnico di Milano, P.zza Leonardo da Vinci 32, 20133 Milano, Italy

[4]Department of Hydrology and Water Resources, The University of Arizona, Tucson, AZ, USA

Abstract

We analyze drawdown reciprocity gaps emerging in interference tests performed in a confined fissured karstic formation. Modeling the system as a dual porosity continuum allows characterizing the dynamics of the relative contribution of the connected fractures and the rock matrix to the total flow rate extracted at the pumping wells. Observed lack of reciprocity of drawdowns can then be linked to the occurrence of processes that are not accounted for in the classical flow models based on a single-continuum representation of the system through flow equations grounded on Darcy's law only. We show that interpreting the system as a dual porosity continuum can cause drawdown reciprocity gaps to emerge as a consequence of local effects associated with an identifiable contribution of the matrix to the total fluid extracted at the well location during pumping. These theoretical results are then employed to identify the contribution to the flow being supplied to the pumping well by the low conductivity matrix constituting the host rock formation, in contrast to that provided by the fractures. An application to data from two interference tests performed at the Hydrogeological Experimental Site (HES) in Poitiers, France, illustrates the approach. We show that, whenever the matrix is assumed to provide a contribution to the total flow rate extracted, non-reciprocity is expected, the latter being linked to the occurrence of a differential drawdown between fracture and matrix at the pumping well. This difference decreases with time in the example presented, displaying a power-law late time behavior, with non-reciprocity effects persisting up to remarkably long times.

Highlights

- Reciprocity gaps of drawdowns can arise in interference tests in fractured media
- Non-reciprocity can be interpreted through a dual porosity flow model
- Reciprocity gaps emerge mathematically depending from the way the pumping well is embedded in the model
- Non-reciprocity informs on dynamics of fracture/matrix contribution to pumping rates

Keywords

Dual porosity model; reciprocity gaps; fractured media; interference pumping tests.

1. Introduction

Conceptual models employed to describe fluid flow in fractured reservoirs include (1) explicit representations of discrete fractures embedded in a rock matrix, (2) the adoption of a single equivalent porous continuum, and (3) the use of multiple continua formulations. Reviews of these and other approaches are included in the works of, e.g., *Berkowitz* [2002], *Neuman* [2005], *Sahimi* [2011], and *Ghasemizadeh et al*. [2012]. Amongst these approaches, we are here concerned with conceptual models based on the depiction of the fractured medium as a system composed by two overlapped continua, according to which a highly conductive medium (representing the collection of fractures in the domain) is embedded within a low conductivity matrix, constituting the host rock. In this context, one can distinguish between dual porosity or dual permeability modeling schemes, depending on whether the host porous rock acts solely as a storage for (or release of) the fluid or also constitutes an active domain for flow. Applications of such models for the analysis and interpretation of fluid flow in natural settings include, amongst others, the works of *Huyakorn et al*. [1983], *Dershowitz and Miller* [1995], *Huang et al*. [2004], *Samardzioska and Popov* [2005], *Maréchal et al*. [2008], *Bailly et al*. [2009], *Trottier et al*. [2014]. Analytical solutions for the interpretation of constant-rate pumping tests in fractured systems have also been developed, relying upon the dual porosity approach associated with pseudo-steady state exchange between fractures and matrix [*De Smedt*, 2011, and references therein].

An interesting feature of dual continua approaches which we investigate in this work is their ability of giving rise to reciprocity gaps when used in the context of numerical modeling of cross-hole pumping tests. In this context, the drawdown evolution as a function of time observed at a location *A* and induced by pumping at a location *B* is said to be reciprocal with that observed in *B* and due to pumping in *A* when

71 these coincide after normalization by the respective flow rates [e.g., *Bruggeman*, 1972;
72 *Raghavan*, 2009, and references therein].

73 Recent studies have analyzed the conditions under which drawdown reciprocity
74 gaps during interference tests can be observed. *Mao et al*. [2013] showed by numerical
75 simulations that reciprocity might not hold for flow in variably saturated media. *Delay*
76 *et al*. [2012] focused on unconfined aquifer systems and found that reciprocity gaps in
77 vertically-averaged drawdowns can be related to the occurrence of (*a*) vertical trends in
78 hydraulic conductivity and/or specific storage, or (*b*) significant drainage from the
79 unsaturated zone. *Delay et al*. [2011] stated that reciprocity of modeled drawdowns is
80 inherently linked to the nature of groundwater flow models in fully saturated media
81 based on Darcian concepts applied to porous or fractured, homogeneous or
82 heterogeneous systems, provided they are represented as a single equivalent continuum.

83 *Delay et al*. [2011] further analyzed the possibility of emergence of reciprocity
84 gaps in the context of dual continua representations of fractured reservoirs. They
85 demonstrated rigorously that, in these settings and under general transient conditions,
86 reciprocity holds only for drawdowns that occur within the fractures. Otherwise,
87 modeled drawdowns in the matrix continuum are generally nonreciprocal. The
88 analytical developments of *Delay et al*. [2011] are based on treating the pumping wells
89 as sink/source terms operating in the fracture continuum.

90 Here, we address the following objectives: (a) to assess the implications on
91 modeled reciprocity gaps of treating the pumping well as a model boundary to the
92 governing dual porosity formulation; and (b) to provide an approach to characterize the
93 way the rock matrix contributes to the global flow rate extracted at the pumping well.
94 We consider these questions by analyzing through a dual porosity model reciprocity
95 gaps observed during standard interference tests in a fractured rock formation. The

96 motivation underlying the study of the first problem is related to the observation that
97 pumping rates are considered as boundary terms in convergent flow scenarios [see, *e.g.*,
98 *De Smedt*, 2011 for a dual porosity setting], while being typically included in standard
99 numerical models of groundwater flows by modeling wells as source/sink terms. It is
100 then relevant to provide an appropriate characterization of the effects that the
101 mathematical representation of an external stress such as pumping can exert on the
102 pressure and flow distributions governed by the model we analyze.

103 A key driver to our study of the second objective is the observation that, while
104 the rock matrix is typically considered to provide only a negligible contribution to the
105 flow rate displaced in the medium, recent studies point out that in some cases the
106 temporal evolution of drawdowns in the vicinity of the pumping well displays a power-
107 law behavior [e.g., *Bogdanov et al*., 2003; *Le Borgne et al*., 2004; *Chang et al*., 2011].
108 We contend that the latter is associated with the joint contribution of the fracture and of
109 the rock matrix to the flow rate extracted at the pumping well.

110 We ground our theoretical analysis on drawdown data collected at the
111 Hydrogeological Experimental Site (HES) in Poitiers, France [*Audouin et al*., 2008;
112 *Riva et al.,* 2009; *Trottier et al.,* 2014]. To the best of our knowledge, this is the first
113 study providing a theoretically rigorous analysis of the information that can be extracted
114 from reciprocity gaps associated with drawdown signals of the kind observed during
115 interference pumping tests in a fractured system with the aim of providing information
116 about the hydraulic behavior of the fractured-matrix medium, with emphasis on the
117 temporal evolution of drawdowns.

118 The work is organized as follows. Section 2 motivates the work through a brief
119 illustration of the HES field site which constitutes an example of a karstified domain
120 where interference tests have been performed and both reciprocal and non-reciprocal

121 drawdown curves have been reported. Section 3 presents the mathematical analyses
122 associated with applications of the reciprocity theorem by considering a cross-hole
123 pumping test in a fractured medium; here flow is interpreted through a dual porosity
124 formulation where the pumping well is treated according to diverse modeling
125 alternatives. This framework is then applied in Section 4 to the analysis of interference
126 tests performed at the site to illustrate our approach for the characterization of the
127 contribution of the rock matrix to the global flow rate extracted from the fractured
128 medium.

129 **2. Reciprocity gaps observed at the HES site**

130 Reciprocal and nonreciprocal drawdown curves were recorded during the
131 interference tests performed at the Hydrogeological Experimental Site (HES) in
132 Poitiers, France. The site has been extensively characterized by exploratory analysis,
133 including geophysical, sedimentological, petrophysical, and hydraulic testing, as
134 documented by *Pourpak et al.* [2009] and *De Dreuzy et al.* [2006]. The host geological
135 system is a fractured medium with the presence of open karstic conduits. Seismic data
136 interpretation suggested that the site can be characterized as a three-dimensional
137 complex system where high porosity bodies are embedded in a low-porosity (compact)
138 matrix, thus supporting a conceptualization of the medium as a dual continuum for the
139 purpose of flow dynamics analyses [e.g., *Kaczmaryk and Delay*, 2007].

140 Interference tests were performed through a standard procedure according to
141 which water is extracted at a constant flow rate from a well and drawdowns are
142 monitored at all other wells. Pumping was performed sequentially at selected wells
143 within the site, each test lasting 60 to 120 h of pumping, followed by a relaxation period
144 of a few days to enable heads to return to their initial levels. Additional test operational
145 details are presented by *Kaczmaryk and Delay* [2007] and *Riva et al*. [2009].

146 An example of observed reciprocal and nonreciprocal drawdowns which can be
147 associated with the same pumping location is depicted in Figure 1. When data from
148 wells P6 and 07 are jointly analyzed, the drawdown curves are starkly reciprocal
149 (Figure 1a). Otherwise, drawdown curves recorded from the interference test performed
150 between wells P6 and 11 (Figure 1b) are nonreciprocal. Viewing the problem through a
151 classical analysis of point-to-point connectivity based on the time elapsed between start
152 of pumping and first response at the observation well [e.g., *Trinchero et al.*, 2008;
153 *Fernandez-Garcia et al.*, 2010], the observed data would imply that P6 is less connected
154 (in hydraulic terms) to 11 than 11 is to P6, (drawdowns in P6 while pumping in P11
155 appear later than drawdowns in P11 when pumping in P6; see Figure 1b).

156 Additional analysis of this observed behavior could be based on the work of
157 *Meier et al*. [1998] and *Sanchez-Vila et al*. [1999]. According to these authors, in a
158 single continuum representation of the system and after long times all drawdown curves
159 should display the same slope when viewed in a drawdown versus log-time plot; such
160 slope is directly related to the effective transmissivity of the site. Figure 1b shows that
161 the slope of the drawdown curve recorded when pumping takes place at point 11
162 displays a late time slope which is higher than that observed when pumping takes place
163 at well P6. On the basis of the results depicted in Figure 1a, the behavior observed in
164 Figure 1b is an additional indication that it is not possible to model the flow response
165 around well 11 as a single continuum.

166 **3. Effect of the Choice of Boundary Conditions at the Pumping Well in a Dual**
167 **Porosity Model for the Characterization of Reciprocity Gaps**

168 We conceptualize a fractured system by means of a dual porosity model. The
169 system of equations driving flow in such a system is

170 $$\nabla\cdot\left(K\nabla\psi^f\right)(\boldsymbol{x},t)=S_s^f(\boldsymbol{x})\frac{\partial\psi^f(\boldsymbol{x},t)}{\partial t}+\sigma(\boldsymbol{x})\left(\psi^f(\boldsymbol{x},t)-\psi^m(\boldsymbol{x},t)\right),\qquad \boldsymbol{x}\in\Omega \tag{1}$$

171 $$S_s^m(\boldsymbol{x})\frac{\partial\psi^m(\boldsymbol{x},t)}{\partial t}=\sigma(\boldsymbol{x})\left(\psi^f(\boldsymbol{x},t)-\psi^m(\boldsymbol{x},t)\right).\qquad \boldsymbol{x}\in\Omega \tag{2}$$

172 Here, superscripts *f* and *m* refer to fracture and matrix continua, respectively; $\psi^i(\boldsymbol{x},t)$
173 (*i*=*f*, *m*) is drawdown [L] at vector location $\boldsymbol{x}$ and time t in the domain Ω, defined as
174 the difference between the initial head and that driven by pumping; $S_s^i(\boldsymbol{x})$ (*i*=*f*, *m*) is
175 specific storage [L^{-1}]; $\sigma(\boldsymbol{x})$ [L^{-1} T^{-1}] is a spatially variable parameter controlling the
176 mass of fluid transferred between fracture and matrix, driven by the pressure/head
177 differences locally existing between the two continua; and $\boldsymbol{u}^f(\boldsymbol{x},t)=K(\boldsymbol{x})\nabla\psi^f(\boldsymbol{x},t)$
178 is the water flux [L T^{-1}], assumed to take place solely in the fractures (notice that from
179 the definition of drawdown, $\nabla\psi(\boldsymbol{x},t)=-\nabla h(\boldsymbol{x},t)$), $K(\boldsymbol{x})$ [L T^{-1}] being hydraulic
180 conductivity of the fracture continuum. Equations (1)-(2) are supplemented by
181 appropriate initial and boundary conditions. Regarding the former, we consider zero
182 initial drawdown at all points, i.e., $\psi^f(\boldsymbol{x},t=0)=\psi^m(\boldsymbol{x},t=0)=0$.

183 We then assume homogeneous boundary conditions at all points along the
184 external domain boundary. As opposed to *Delay et al.* [2011], we explicitly treat the
185 pumping well as an internal boundary, where the volume of water pumped is given as
186 the sum of the volume extracted directly from the fracture and that supplied from the
187 matrix, i.e.,

188 $$-\int_{\partial\Omega}K(\boldsymbol{x})\frac{\partial\psi^f}{\partial r}(\boldsymbol{x},t)\,d\Gamma+\int_{\partial\Omega}\alpha(\boldsymbol{x})\left(\psi^f(\boldsymbol{x},t)-\psi^m(\boldsymbol{x},t)\right)d\Gamma=Q_w(t), \tag{3}$$

189 $Q_w(t)$ and $\partial\Omega$ respectively being the pumping rate taking place at the well, and the
190 surface area of the well boundary; here, purely convergent flow is assumed in the close
191 proximity of the well. Note that cylindrical coordinates are implied, i.e., $\boldsymbol{x} = (r, \theta, z)$, in
192 (3) and in all subsequent equations with the origin of coordinates always centered at the
193 selected pumping well. The sign convention adopted implies that Q_w is positive when
194 drawdown is positive (i.e., water is extracted from the well). The quantity $\alpha(\boldsymbol{x})$ [T^{-1}]
195 in (3) deserves some comments. The model considers that the flow rate at the well is
196 supplied by the joint effects of the head (or drawdown) gradient within the fracture
197 continuum and the head/drawdown difference between the two continua (fracture and
198 matrix), $\alpha(\boldsymbol{x})$ being a parameter indicating the potential of the matrix to contribute to
199 the total flow extracted. This contribution is directly related to the local (i.e., at the well
200 location) value of $\sigma(\boldsymbol{x})$, as well as to the radius of the well, r_w. As an example,
201 assuming that σ and drawdown values are uniform along the vertical at the well
202 location, and after some algebra, it can be shown from (3) that $\alpha = \frac{1}{2}\sigma r_w$.

203 As $\boldsymbol{u}^f(\boldsymbol{x},t)$ is linearly proportional to the drawdown gradient, it is possible to
204 apply Lorentz's principle of reciprocity between ψ^f and the Hermitian operator $\nabla\cdot\nabla$.
205 Casting the problem in Laplace space allows writing the principle of reciprocity as

206
$$\begin{aligned}&\int_{\Omega}\left(\nabla\cdot\tilde{\boldsymbol{u}}_A^f(\boldsymbol{x},s)\tilde{\psi}_B^f(\boldsymbol{x},s)-\nabla\cdot\tilde{\boldsymbol{u}}_B^f(\boldsymbol{x},s)\tilde{\psi}_A^f(\boldsymbol{x},s)\right)d\Omega=\\&\int_{\partial\Omega}\left(\tilde{\boldsymbol{u}}_B^f(\boldsymbol{x},s)\tilde{\psi}_A^f(\boldsymbol{x},s)-\tilde{\boldsymbol{u}}_A^f(\boldsymbol{x},s)\tilde{\psi}_B^f(\boldsymbol{x},s)\right)\cdot\boldsymbol{n}\,d\Gamma,\end{aligned}\qquad(4)$$

207 where, $\psi_j^f(\boldsymbol{x},t)$ and $\boldsymbol{u}_j^f(\boldsymbol{x},t)$ respectively are drawdown and flux associated with the
208 fracture continuum when pumping is performed at location $j = A, B$; $\boldsymbol{n}$ is the unit vector

normal to the well surface (positive outward); superscript ˜ indicates that the corresponding function is expressed in Laplace space, s being the Laplace parameter. It can be shown that the left hand side of (4) vanishes (see Appendix A). Thus,

$$\int_{\partial\Omega} \tilde{\psi}_A^f(\boldsymbol{x},s)\tilde{\boldsymbol{u}}_B^f(\boldsymbol{x},s)\cdot\boldsymbol{n}\,d\Gamma = \int_{\partial\Omega} \tilde{\psi}_B^f(\boldsymbol{x},s)\tilde{\boldsymbol{u}}_A^f(\boldsymbol{x},s)\cdot\boldsymbol{n}\,d\Gamma\,. \tag{5}$$

Note that (5) is characterized by one well being active, extracting a flow rate $Q_j(t)$ (j = A, B), the other one being inactive. Rewriting (5), introducing the corresponding subscripts in Ω, Γ to denote that the integrals are performed at the well locations (either A or B), yields

$$\int_{\partial\Omega_B} \tilde{\psi}_A^f(\boldsymbol{x},s)K(\boldsymbol{x})\frac{\partial\tilde{\psi}_B^f(\boldsymbol{x},s)}{\partial r}d\Gamma_B = \int_{\partial\Omega_A} \tilde{\psi}_B^f(\boldsymbol{x},s)K(\boldsymbol{x})\frac{\partial\tilde{\psi}_A^f(\boldsymbol{x},s)}{\partial r}d\Gamma_A\,. \tag{6}$$

Finally, introducing the boundary conditions (3) for wells A and B, respectively pumped at flow rates Q_A and Q_B, assuming that the drawdown in the fracture continuum is uniform along open boreholes at the observation location, and that the difference $\left(\psi^f(\boldsymbol{x},t)-\psi^m(\boldsymbol{x},t)\right)$ is relatively uniform along the pumped borehole, leads to

$$\begin{aligned}&\tilde{\psi}_B^f(\boldsymbol{x}_A,s)\left(\tilde{Q}_A(s)-\mu_A\left(\tilde{\psi}_A^f(\boldsymbol{x}_A,s)-\tilde{\psi}_A^m(\boldsymbol{x}_A,s)\right)\right)=\\&\tilde{\psi}_A^f(\boldsymbol{x}_B,s)\left(\tilde{Q}_B(s)-\mu_B\left(\tilde{\psi}_B^f(\boldsymbol{x}_B,s)-\tilde{\psi}_B^m(\boldsymbol{x}_B,s)\right)\right),\end{aligned} \tag{7}$$

where $\mu_j = \int_{\partial\Omega_j} \alpha(\boldsymbol{x})\,d\Gamma$, ($j$ = A, B).

As opposed to the results of *Delay et al.* [2011] associated with a single continuum, here we find from (7) that in general $\tilde{Q}_A(s)\tilde{\psi}_B^f(\boldsymbol{x}_A,s) \neq \tilde{Q}_B(s)\tilde{\psi}_A^f(\boldsymbol{x}_B,s)$. Therefore, reciprocity of drawdowns observed in the fractures is not guaranteed with the exception of the special case where $\mu_A = \mu_B = 0$, or when the drawdowns in the fracture and matrix coincide at all times, the latter condition being representative of a very fast

exchange between the two continua (i.e., the dual continua medium is effectively behaving as a single continuum).

The solution presented in (7) is thus linked to our choice of boundary condition according to which one models the pumping well. A different scheme was investigated by *Delay et al*. [2011], who represent the well as a sink/source term operating in the fracture continuum. By relying on this choice, considering homogeneous initial conditions and casting the problem in Laplace space, *Delay et al*. [2011] found (see their equations (30) and (36b), as well as Appendix A),

$$\tilde{Q}_A(\boldsymbol{x}_A,s)\tilde{\psi}_B^f(\boldsymbol{x}_A,s)-\int_\Omega \sigma(\boldsymbol{x})\tilde{\psi}_A^m(\boldsymbol{x},s)\tilde{\psi}_B^f(\boldsymbol{x},s)d\Omega = \tilde{Q}_B(\boldsymbol{x}_B,s)\tilde{\psi}_A^f(\boldsymbol{x}_B,s)-\int_\Omega \sigma(\boldsymbol{x})\tilde{\psi}_B^m(\boldsymbol{x},s)\tilde{\psi}_A^f(\boldsymbol{x},s)d\Omega \quad (8a)$$

$$\tilde{\psi}_j^m(\boldsymbol{x},s)=\frac{\beta(\boldsymbol{x})}{s+\beta(\boldsymbol{x})}\tilde{\psi}_j^f(\boldsymbol{x},s) \quad , \quad (8b)$$

where $\beta(\boldsymbol{x})=\sigma(\boldsymbol{x})/S_s^m(\boldsymbol{x})$, $\tilde{Q}_j$ being the Laplace transform of the flow rate pumped from the fracture continuum at location $\boldsymbol{x}_j$ (j = A, B). Substitution of (8b) in (8a) yields $\tilde{Q}_A(\boldsymbol{x}_A,s)\tilde{\psi}_B^f(\boldsymbol{x}_A,s)=\tilde{Q}_B(\boldsymbol{x}_B,s)\tilde{\psi}_A^f(\boldsymbol{x}_B,s)$ so that reciprocity of drawdowns in the fracture continuum holds when withdrawal histories at A and B are proportional, *i.e.*, $Q_A(\boldsymbol{x}_A,t)=cQ_B(\boldsymbol{x}_B,t)$, c being a constant.

Comparison of (7) and (8) suggests that in a dual porosity model treating the well either as a source/sink term in the fracture or as a boundary condition (in the way we do in (3)) leads to diverse interpretations of conditions of occurrence of reciprocity gaps as well as to diverse quantifications of the temporal dynamics of such gaps, as driven by the conceptual model employed for the representation of the medium.

4. Characterization of Rock Matrix Contribution to Total Extracted Flow Rate

Here, we explore the application of (7) to provide information about the way the rock matrix contributes to the global flow rate conveyed through the medium in the modeling context analyzed. We start by noting that in interference tests the observables are the flow rate and drawdowns at the pumping and observation boreholes [e.g., *Illman*, 2014 and references therein]. We employ here the common assumption [e.g., *Bourbiaux*, 2010] that a measurement device (e.g., a pressure transducer) placed at a borehole provides information mostly about the drawdown at the fracture. As such, corresponding drawdowns in the matrix cannot be properly measured in general and might only be inferred indirectly.

Thus, in a classical interference test between locations *A* and *B*, measurements of $\tilde{Q}_A(s)$, $\tilde{Q}_B(s)$, $\tilde{\psi}_A^f(\boldsymbol{x}_A,s)$, $\tilde{\psi}_B^f(\boldsymbol{x}_A,s)$, $\tilde{\psi}_A^f(\boldsymbol{x}_B,s)$, and $\tilde{\psi}_B^f(\boldsymbol{x}_B,s)$ are typically available. The coefficients μ_A, μ_B in (7) and the functions $\tilde{\psi}_A^m(\boldsymbol{x}_A,s)$, $\tilde{\psi}_B^m(\boldsymbol{x}_B,s)$, representing drawdowns in the matrix at locations where pumping takes place, are typically unknown. Each additional pumping/observation point included would result in an additional set of unknown quantities, which are given by the corresponding values of μ and $\tilde{\psi}^m$. On these bases, we explore, through observations from the field scale interference pumping test illustrated in Section 2, the way the analysis of detected reciprocity gaps can lead to characterizing the contribution of the matrix to the flow rate extracted at the well.

We recall here Figure 1a, i.e., the drawdown curves recorded at wells P6 and 07 during the interference test. In this case, the drawdown curves display a clear reciprocal behavior. When this observation is implemented in (7), it is concluded that

$$\mu_j\left(\tilde{\psi}_j^f\left(\boldsymbol{x}_j,s\right)-\tilde{\psi}_j^m\left(\boldsymbol{x}_j,s\right)\right)=0, \qquad (j = \text{P6, 07}). \tag{9}$$

We note that emergence of reciprocity does not necessarily imply that the system should be interpreted as a single continuum. In the context of a dual porosity formulation, it could imply that the flow extracted at the well location is supplied by the fractures in the system, with zero or very limited contribution from the matrix (see (8) and associated discussion). However, a non-reciprocal behavior was observed for the drawdowns recorded in the interference test performed between wells P6 and 11 (Figure 1b).

To interpret the nonreciprocal drawdown curves in Figure 1b, we start by combining (7) and (9), to obtain

$$\frac{\tilde{\psi}_{11}^{f}\left(\boldsymbol{x}_{P6},s\right)}{\tilde{\mathrm{Q}}_{11}\left(s\right)}=\frac{\tilde{\psi}_{P6}^{f}\left(\boldsymbol{x}_{11},s\right)}{\tilde{\mathrm{Q}}_{P6}\left(s\right)}\left[1-\frac{1}{\tilde{\mathrm{Q}}_{11}\left(s\right)}\mu_{11}\left(\tilde{\psi}_{11}^{f}\left(\boldsymbol{x}_{11},s\right)-\tilde{\psi}_{11}^{m}\left(\boldsymbol{x}_{11},s\right)\right)\right], \tag{10}$$

where the subscripts for drawdowns $\tilde{\psi}$ and parameters μ and Q refer to the pumped well, while those for $\boldsymbol{x}$ denote location where the observation took place (either pumping or observation points).

Equation (10) should enable us to estimate μ_{11} and $\tilde{\psi}_{11}^{m}\left(\boldsymbol{x}_{11},s\right)$ if all remaining quantities were available. Drawdowns measured at the pumping wells could not be used at HES, as head losses could not be filtered from the signal at the pumping location, as it is common in most practical applications. As a consequence, the joint use of (10) and available data allows estimating solely the product $\mu_{11}\left(\tilde{\psi}_{11}^{f}\left(\boldsymbol{x}_{11},s\right)-\tilde{\psi}_{11}^{m}\left(\boldsymbol{x}_{11},s\right)\right)$.

Both tests were performed with constant pumping rates, $Q_j(t)=Q_j\,H(t)$ (Q_j = 62.8 or 59.0 $m^3\ h^{-1}$, respectively for j = P6 or 11), $H(t)$ being the Heaviside function. The corresponding Laplace transform is $\tilde{\mathrm{Q}}_j\left(s\right)=\tilde{\mathrm{Q}}_j\left(s\right)=Q_j/s$. Applying Laplace transform to the drawdown data, and assuming these represent those of the fractures, we

295 can then get $\tilde{\psi}_{11}^{f}(\boldsymbol{x}_{P6},s)$ and $\tilde{\psi}_{P6}^{f}(\boldsymbol{x}_{11},s)$, as depicted in Figure 2. Figure 3 depicts the

296 function $\mu_{11}\left(\tilde{\psi}_{11}^{f}(\boldsymbol{x}_{11},s)-\tilde{\psi}_{11}^{m}(\boldsymbol{x}_{11},s)\right)$, as calculated from (10). A regression line

297 obtained as best fit of the data for low *s* values (corresponding to long times) is also

298 depicted. From Figure 3, and noticing that μ_{11} is a constant, one obtains

299 $$\left(\tilde{\psi}_{11}^{f}(\boldsymbol{x}_{11},s)-\tilde{\psi}_{11}^{m}(\boldsymbol{x}_{11},s)\right)\sim s^{-\beta}, \tag{11}$$

300 associated with an estimate of $\beta = 0.82$ (obtained on the basis of visual inspection). As a

301 consequence, the difference between drawdowns observed within the fracture and

302 matrix continua at the pumping well in real space displays a power-law behavior,

303 $$\left(\tilde{\psi}_{11}^{f}(\boldsymbol{x}_{11},t)-\tilde{\psi}_{11}^{m}(\boldsymbol{x}_{11},t)\right)\sim t^{(\beta-1)}, \tag{12}$$

304 where the exponent in the power-law results in $t^{-0.18}$ indicating that the difference tends

305 to vanish for (very) long times. The asymptotic behavior we document suggests that

306 reciprocity gaps associated with an interpretation based on a dual porosity model upon

307 treating the pumping well as a boundary condition tend to disappear for long pumping

308 times, in agreement with the conceptual picture presented by *Acuna et al.* [1995], *Acuna*

309 *and Yortsos* [1995], and *Delay et al*. [2011]. Yet, these gaps remain for very long times

310 in practical applications of the kind we analyzed here.

311 As discussed in Section 3, reciprocity in the fracture drawdowns takes place

312 whenever water is only extracted from the fracture, even as a dual continuum

313 conceptual model is invoked to depict the system behavior, provided that

314 $Q_A(\boldsymbol{x}_A,t)=cQ_B(\boldsymbol{x}_B,t)$. Here we showed that whenever it is considered that the matrix

315 partially contributes to the total flow rate extracted, nonreciprocity is expected, as

316 linked to the occurrence of a differential drawdown between fracture and matrix. This

317 difference decreases with time in the example presented, displaying a power-law late
318 time behavior, characterized by a small (negative) exponent.

319 **4. Conclusions**

320 Our work leads to the following major conclusions:

321 1. We show that interpreting a fractured medium as a dual porosity continuum can
322 cause reciprocal and nonreciprocal behavior of drawdown in modeled interference
323 tests to coexist in a given area, as these are related to the local ability of the matrix
324 to contribute to the total flow extracted at the pumping well.
325 2. We demonstrate that the way the pumping well is treated in a dual porosity model
326 (i.e., as a source/sink term acting in the fracture or as a prescribed flow rate
327 boundary, where the contribution of the matrix to the extracted flow rate is
328 included) has a significant impact on the way reciprocity gaps can emerge and be
329 quantified in the fracture continuum. In this modeling context, absence of drawdown
330 reciprocity gaps might suggest that water is extracted from the fractures, with no
331 contribution from the matrix. That is, the occurrence of reciprocal drawdowns does
332 not necessarily imply that the system behaves as a single continuum so that a dual
333 continuum conceptualization can still form the basis for the description of the flow
334 features in a fractured host formation.
335 3. We explore and quantify for the first time the asymptotic (for long observation
336 times) behavior at the pumping well of the difference between drawdowns
337 associated with the fracture and matrix continua in a dual porosity representation of
338 fractured geological media subject to interference hydraulic tests. Our theoretical
339 results are employed to identify the matrix contribution to the flow being supplied to
340 the pumping well by the host rock formation. This identification is based on actual
341 data from an interference test performed at a fissured confined karstic formation

(HES Site, France). We show that whenever the matrix is assumed to provide a contribution to the total flow rate extracted (a) the resulting non-reciprocity of drawdowns can be employed to quantify such contribution, and (b) the difference between the drawdowns in the fracture and rock continua at the well tends to decrease by following a power-law late time behavior, with non-reciprocity effect persisting up to very long times.

Appendix A

The starting point is the coupled system of partial differential equations given in (1)-(2). Rewriting these equations in Laplace space leads to

$$\nabla\cdot\tilde{\boldsymbol{u}}^f\left(\boldsymbol{x},s\right)=sS_s^f\left(\boldsymbol{x}\right)\tilde{\psi}^f\left(\boldsymbol{x},s\right)+\sigma\left(\boldsymbol{x}\right)\left(\tilde{\psi}^f\left(\boldsymbol{x},s\right)-\tilde{\psi}^m\left(\boldsymbol{x},s\right)\right), \tag{A.1}$$

$$sS_s^m\left(\boldsymbol{x}\right)\tilde{\psi}^m\left(\boldsymbol{x},s\right)=\sigma\left(\boldsymbol{x}\right)\left(\tilde{\psi}^f\left(\boldsymbol{x},s\right)-\tilde{\psi}^m\left(\boldsymbol{x},s\right)\right). \tag{A.2}$$

From (A.2) we obtain

$$\tilde{\psi}^m\left(\boldsymbol{x},s\right)=\frac{\beta\left(\boldsymbol{x}\right)}{s+\beta\left(\boldsymbol{x}\right)}\tilde{\psi}^f\left(\boldsymbol{x},s\right), \tag{A.3}$$

where $\beta\left(\boldsymbol{x}\right)=\sigma\left(\boldsymbol{x}\right)/S_s^m\left(\boldsymbol{x}\right)$. Replacing (A.3) into (A.1) leads to

$$\nabla\cdot\tilde{\boldsymbol{u}}^f\left(\boldsymbol{x},s\right)=sS_s^f\left(\boldsymbol{x}\right)\tilde{\psi}^f\left(\boldsymbol{x},s\right)+\frac{s\sigma\left(\boldsymbol{x}\right)}{s+\beta\left(\boldsymbol{x}\right)}\tilde{\psi}^f\left(\boldsymbol{x},s\right). \tag{A.4}$$

One can then evaluate the left hand side of (5) through the use of (A.4)

$$\begin{aligned}&\int_\Omega\left(\nabla\cdot\tilde{\boldsymbol{u}}_A^f\left(\boldsymbol{x},s\right)\tilde{\psi}_B^f\left(\boldsymbol{x},s\right)-\nabla\cdot\tilde{\boldsymbol{u}}_B^f\left(\boldsymbol{x},s\right)\tilde{\psi}_A^f\left(\boldsymbol{x},s\right)\right)d\Omega=\\&\int_\Omega\left[\begin{array}{l}\left(sS_s^f\left(\boldsymbol{x}\right)\tilde{\psi}_A^f\left(\boldsymbol{x},s\right)+\dfrac{s\sigma\left(\boldsymbol{x}\right)}{s+\beta\left(\boldsymbol{x}\right)}\tilde{\psi}_A^f\left(\boldsymbol{x},s\right)\right)\tilde{\psi}_B^f\left(\boldsymbol{x},s\right)\\-\left(sS_s^f\left(\boldsymbol{x}\right)\tilde{\psi}_B^f\left(\boldsymbol{x},s\right)+\dfrac{s\sigma\left(\boldsymbol{x}\right)}{s+\beta\left(\boldsymbol{x}\right)}\tilde{\psi}_B^f\left(\boldsymbol{x},s\right)\right)\tilde{\psi}_A^f\left(\boldsymbol{x},s\right)\end{array}\right]d\Omega=0\end{aligned} \tag{A.5}$$

Acknowledgements

AG acknowledges funding from MIUR (Italian ministry of Education, Universities and Research- PRIN2010-11; project: "Innovative methods for water resources under hydro-climatic uncertainty scenarios"). XS acknowledges funding from the ICREA Academia Program and from the EU 7th Framework Programme for Research, Technological Development and Demonstration, grant agreement 619120 (project MARSOL). The authors commit to make their data available and refer the reader to the corresponding author.

References

Acuna, J.A., I. Ershaghi, Y.C. Yortsos (1995) Practical applications of fractal pressure transient analysis of naturally fractured reservoirs, *SPE Form Eval*., 173-179.

Acuna, J.A., Y.C. Yortsos (1995) Application of fractal geometry to the study of networks of fractures and their pressure transient, *Water Resour. Res*., 31(3), 527-540.

Audouin, O., J. Bodin, G. Porel, B. Bourbiaux (2008) Flowpath structure in a limestone aquifer: Multi-borehole logging investigations at the hydrogeological experimental site of Poitiers, France, *Hydrogeol. J*., 16(5), 939-950.

Bailly, D., R. Ababou, M. Quintard (2009) Geometric characterization, hydraulic behavior and upscaling of 3-D fissured geologic media, *Math. Comput. in Sim*., 79, 3385-3396.

Berkowitz, B. (2002) Characterizing flow and transport in fractured geological media: A review, *Advances Water Resour*., 25, 861-884.

Bogdanov, I.I., V.V. Mourzenko, J.-F. Thovert, P.M. Adler (2003) Pressure drawdown well tests in fractured porous media, *Water Resour. Res*., 39(1), doi: 10.1029/2000WR000080.

384 Bourbiaux, B. (2010) Fractured reservoir simulations: a challenging and rewarding
385 issue, *Oil & Gas Sci. Technol.*, 65(2), 227-238, doi:10.2516/ogst/2009063.
386 Bruggeman, G.A. (1972) The reciprocity principle in flow through heterogeneous
387 porous media, Fundamentals of transport in porous media, IAHR Publications,
388 Elsevier, Amsterdam, 135-149.
389 Chang, Y.-C., H.-D. Yeh, K.-F. Liang, M.-C.T. Kuo (2011) Scale dependency of
390 fractional flow dimension in a fractured formation, *Hydrol. Earth Syst. Sci.*, 15,
391 2165-2178, doi:10.5194/hess-15-2165-2011.
392 De Dreuzy, J.R., J. Bodin, H. Le Grand, P. Davy, D. Boulanger, A. Battais, O. Bour, P.
393 Gouze, G. Porel (2006) General database for ground water site information,
394 *Ground Water*, 44 (5), 743-748.
395 De Smedt, M. (2011) Analytical solution for constant-rate pumping test in fissured
396 porous media with Double-Porosity behaviour, *Trasp. Porous Med.*, 88, 479-489,
397 doi:10.1007/s11242-011-9750-9.
398 Delay, F., P. Ackerer, A. Guadagnini (2011) Theoretical analysis and field evidence of
399 reciprocity gaps during interference pumping tests. *Adv. Water Resour.*, 34(5), 592-
400 606, doi:10.1016/j.advwatres.2011.02.006.
401 Delay, F., P. Ackerer, B. Belfort, A. Guadagnini (2012) On the emergence of
402 reciprocity gaps during interference pumping tests in unconfined aquifers, *Adv.*
403 *Water Resour.*, 46, 11-19, doi:10.1016/j.advwatres.2012.06.002.
404 Dershowitz, W., I. Miller (1995) Dual porosity fracture flow and transport, *Geophys.*
405 *Res. Lett.*, 22(11), 1441-1444.
406 Fernandez-Garcia, D., P. Trinchero, X. Sanchez-Vila (2010) Conditional stochastic
407 mapping of transport connectivity, *Water Resour. Res.*, 46, W10515,
408 doi:10.1029/2009WR008533.

409 Ghasemizadeh, R., F. Hellweger, C. Butscher, I. Padilla, D. Vesper, M. Field, A.
410 Alshawabkeh (2012) Review: Groundwater flow and transport modeling of karst
411 aquifers, with particular reference to the North Coast Limestone aquifer system of
412 Puerto Rico, *Hydrogeol J*., 20(8), 1441-1461, doi: 10.1007/s10040-012-0897-4.
413 Huang, W., G. Di Donato, M.J. Blunt (2004) Comparison of streamline-based and grid-
414 based dual porosity simulations, *Soc. Petrol. Eng. J*, 43(2), 129-137.
415 Huyakorn, P.S., B.H. Lester, C.R. Faust (1983) Finite element technique for modeling
416 groundwater flow in fractured aquifers, *Water Resour. res*., 19(4), 1019-1035.
417 Illman, W.A. (2014) Hydraulic tomography offers improved imaging of heterogeneity
418 in fractured rocks, *Groundwater*, 52(5), 659-684, doi:10.1111/gwat.12119.
419 Kaczmaryk, A., F. Delay (2007) Interpretation of interference pumping test in fractured
420 limestone by means of dual-medium approaches, *J. Hydrol*., 337, 133-146,
421 doi:10.1016/j.jhydrol.2007.01.004.
422 Le Borgne, T., J.R., De Dreuzy, P. Davy, F. Touchard (2004) Equivalent mean flow
423 models for fractured aquifers: Insights from a pumping tests scaling interpretation,
424 *Water Resour. Res*., 40, W03512, doi:10.1029/2003WR002436.
425 Mao, D., T.-C.J. Yeh, L. Wan, C.-H. Lee, K.-C. Hsu, J.-C. Wen, W. Lu (2013) Cross-
426 correlation analysis and information content of observed heads during pumping in
427 unconfined aquifers, *Water Resour. Res*., 49, 713-731, doi:10.1002/wrcr.20066.
428 Maréchal, J.-C., B. Ladouche, N. Dörfliger, P. Lachassagne (2008) Interpretation of
429 pumping tests in a mixed flow karst system, *Water Resour. Res*., 44, W05401,
430 doi:10.1029/2007WR006288.
431 Meier, P.M., J. Carrera, X. Sanchez-Vila (1998) An evaluation of Jacob's method for
432 the interpretation of pumping tests in heterogeneous formations, *Water Resour.*
433 *Res*., 34(5), 1011-1025, doi:10.1029/98WR00008.

434 Neuman, S.P. (2005) Trends, prospects and challenges in quantifying flow and transport
435 through fractured rocks, *Hydrogeol. J.*, 13, 124-147.
436 Pourpak, H., B. Bourbiaux, F. Roggero, F. Delay (2009) An integrated methodo-logy
437 for calibrating a heterogeneous fractured reservoir model from wellbore flow
438 measurements: Case study, *Soc. Petrol. Eng.*, SPE-113528, 433-445.
439 Raghavan, R. (2009) Complex geology and pressure tests, *J Petrol Sci Eng*, 69, 181-
440 188.
441 Riva, M., A. Guadagnini, J. Bodin, F. Delay (2009) Characterization of the
442 Hydrogeological Site of Poitiers–France by stochastic well testing analysis, *J.*
443 *Hydrol.*, 369, 154-164, doi:10.1016/j.jhydrol.2009.02.040.
444 Sahimi, M. (2011) *Flow and Transport in Porous Media and Fractured Rocks*, Wiley,
445 709 p.
446 Samardzioska, T., V. Popov (2005) Numerical comparison of the equivalent continuum,
447 non-homogeneous and dual porosity models for flow and transport in fractured
448 porous media, *Advances Water Resour.*, 28, 235-255.
449 Sanchez-Vila, X., P.M. Meier, J. Carrera (1999) Pumping tests in heterogeneous
450 aquifers: An analytical study of what can be obtained from their interpretation
451 using Jacob's method, *Water Resour. Res.*, 35(4), 943-952,
452 doi:10.1029/1999WR900007.
453 Teutsch, G. (1989) Groundwater models in karstified terrains: two practical examples
454 from the Swabian Alb, S. Germany. Proc. 4th Conference - Solving Groundwater
455 Problems with Models (Indianapolis, USA, 1989), 929-953.
456 Trinchero, P., X. Sanchez-Vila, D. Fernandez-Garcia (2008) Point-to-point
457 connectivity, an abstract concept or a key issue for risk assessment studies?, *Adv.*
458 *Water Res.*, 31(12), 1742-1753, doi:10.1016/j.advwatres.2008.09.001.

459 Trottier, N., F. Delay, O. Bildstein, P Ackerer (2014) Inversion of a dual-continuum
460 approach to flow in a karstified limestone: Insight into heterogeneity revealed by
461 well-test interferences, *J. Hydrol.*, 508, 157-169.
462

Figures

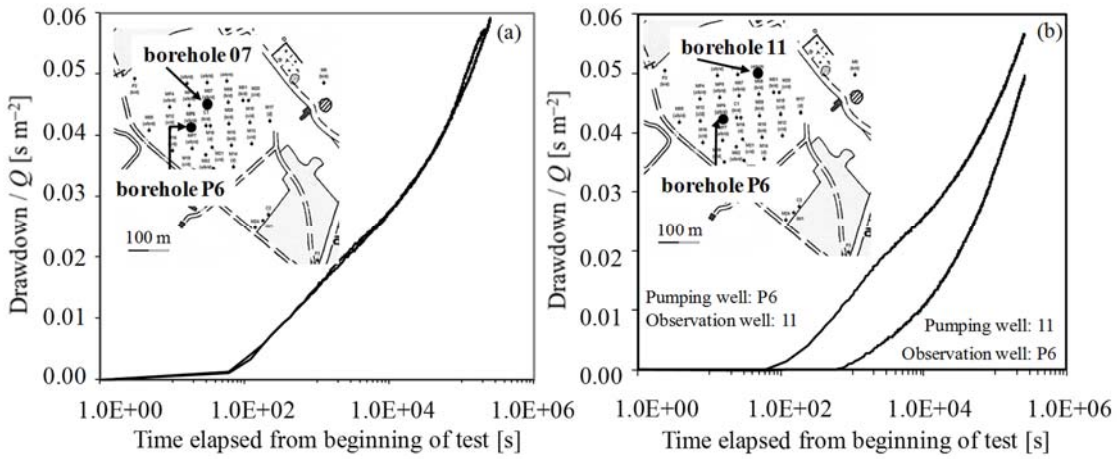

Figure 1. Drawdown curves observed during interference pumping tests performed at the Hydrogeological Experimental Site (HES): (a) example of reciprocity detected between wells P6 and 07; (b) example of observed reciprocity gaps between wells P6 and 11. Figure adapted from *Delay et al*. [2011].

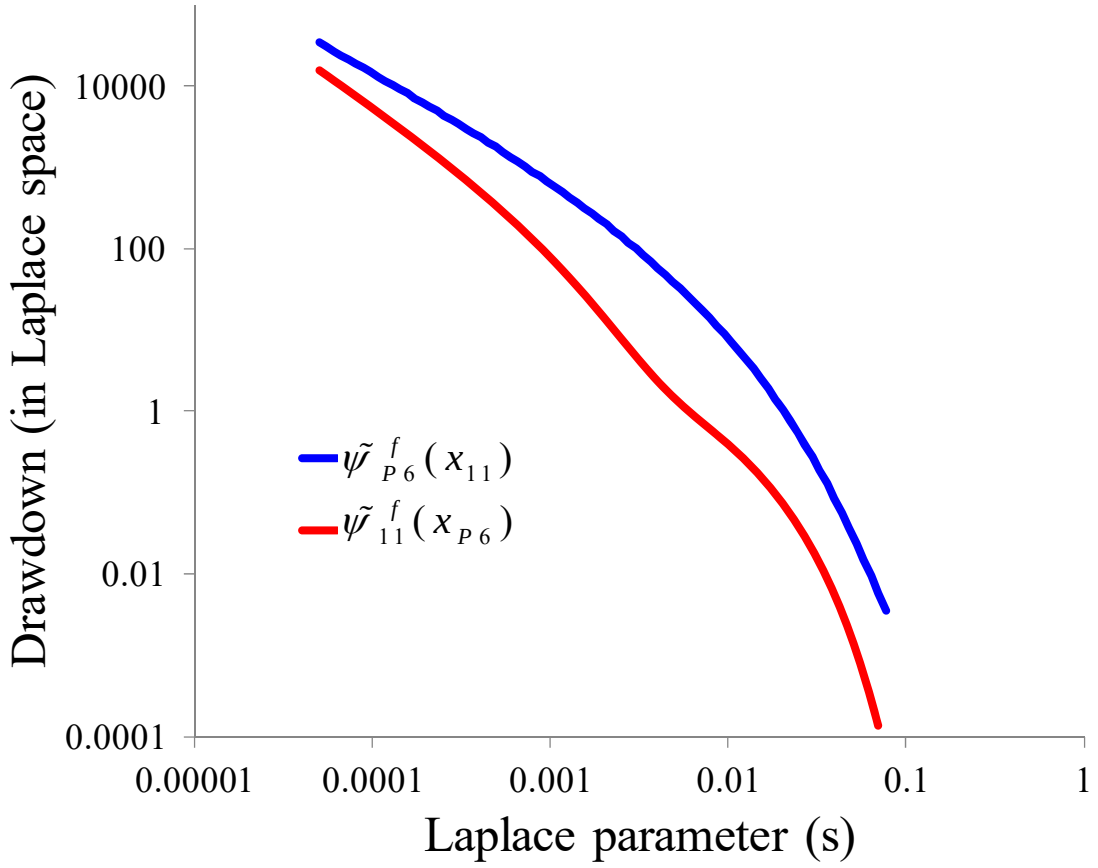

471

472 Figure 2. Discrete Laplace transform of the drawdown data observed at well 11 when
473 pumping is performed at well P6 (in blue) and of drawdowns measured at P6 when
474 pumping in 11 (in red). Curves are constructed by transforming the drawdown data
475 depicted in Figure 1b to Laplace space.

476

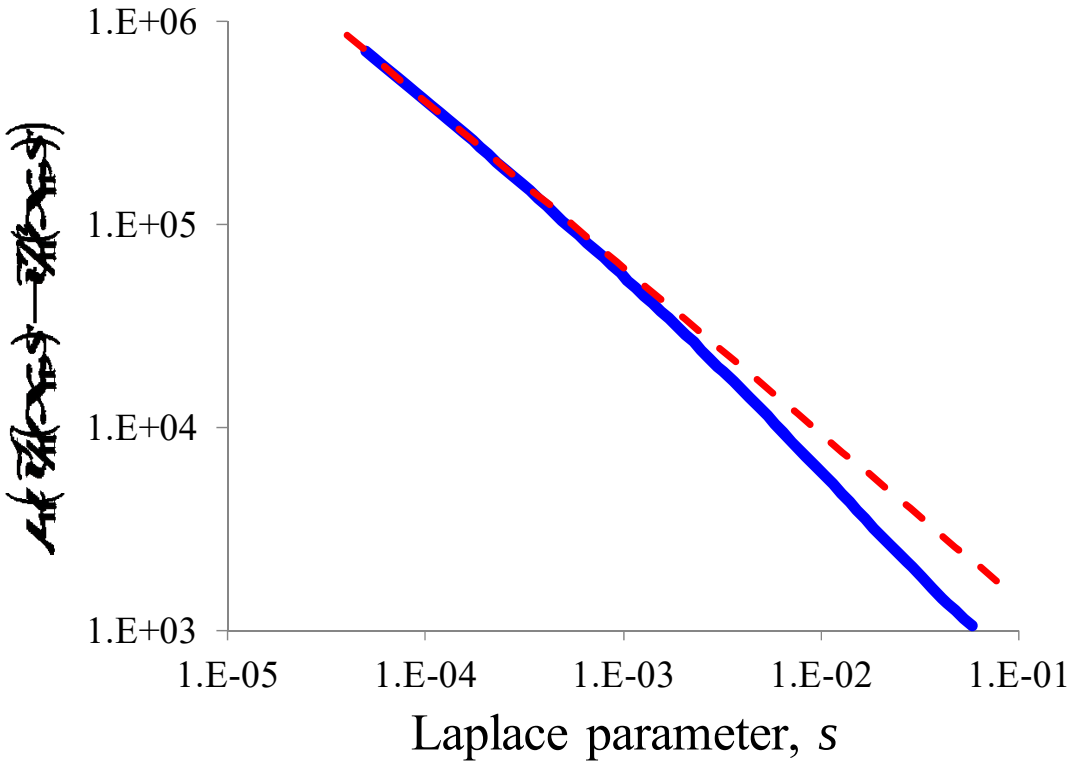

477

478 Figure 3. Blue (solid) curve: estimate of the fracture-matrix drawdown differential,

479 $\mu_{11}\left(\tilde{\psi}_{11}^{f}(\boldsymbol{x}_{11},s)-\tilde{\psi}_{11}^{m}(\boldsymbol{x}_{11},s)\right)$, based on the data from the test depicted in Figure 2 and

480 (9); red (dashed) line: best linear estimate (in log-log space) obtained using only data

481 for small values of the Laplace parameter s, indicating a power-law behavior.